INFLUENCE OF RELIEF ON THE ATMOSPHERIC ELECTRIC FIELD

V.V. Denisenko
Institute of Computational Modelling SB RAS,
Krasnoyarsk, Russia, denisen@icm.krasn.ru

Abstract. Measurements of the fair-weather electric field in mountainous areas are affected by the terrain, and therefore need additional calibration to be included in the global field picture. To do this, it is proposed to solve the three-dimensional electric current continuity problem of the atmosphere in the region between the Earth surface and the ionosphere. As an example, the neighborhood of Klyuchevskaya Sopka is considered. With an increase in the height of the plateaus, the fair-weather electric current density above them increases, and the electric field strength decreases. A one-dimensional model of atmospheric conductivity is not applicable for the terrain with steep slopes. A comparison of the daily-seasonal diagrams constructed according to the data from Carnegie Cruise VII and from the Tomsk Observatory has shown that the fair-weather electric field strength variations are similar in such different places on Earth. The field over the sea is about half as small as over low-lying land at the same time.

Keywords: atmosphere, global electric circuit, fair-weather electric field, calibration, relief, daily-seasonal diagram.

INTRODUCTION

In the last decade, there has been a growing interest in studying processes in the global electric circuit (GEC). According to present-day views [Mareev, 2010], GEC currents are generated in thunderstorm and electrified clouds. An external electric current flowing upward inside a cloud is closed by conduction currents inside and outside the cloud. In the latter case, part of the conduction current goes above the cloud into the ionosphere, spreads over it, flows globally throughout the atmosphere down to the Earth surface, accumulates near the region under the cloud, and through the lower atmosphere reaches the cloud base. At the same time, the characteristic potential difference between the Earth surface and the ionosphere, which determines the electric field throughout the atmosphere, is 300 kV. In the air near the ground far away from clouds, the electric field strength is 100–200 V/m. Such a field is called a fair-weather electric field. Measuring the field is a challenging task, which is even more complicated if an observatory is not located on a plain.

The purpose of this work is to study the influence of local relief on the fair-weather field and to develop a measurement calibration method that allows us to avoid local features, which is necessary for using measurement data in the global pattern of GEC.

1. ATMOSPHERIC CONDUCTOR

When describing electrical processes in the atmosphere, the characteristic time of which exceeds 15 min, a quasi-stationary model can be adopted [Molchanov, Hayakawa, 2008]. The basic equations for the stationary electric field strength **E** and the current density **j** are the Faraday law, the charge conservation law, and the Ohm law $\mathbf{j}=\sigma\mathbf{E}$. We can introduce an electric potential V so that $\mathbf{E}=-\mathrm{grad}\,V$. Then the system of equations reduces to the electric current continuity equation

$$-\mathrm{div}\left(\sigma\,\mathrm{grad}\,V\right)=0, \tag{1}$$

where σ is the air conductivity whose spatial distribution is assumed to be given. The surface air conductivity is much lower than that of soil and seawater. The Earth surface is, therefore, usually considered as an ideal conductor. Since the ionosphere conductivity is many orders of magnitude higher than that of the atmosphere, the ionosphere can also be considered as an ideal conductor when modeling the atmosphere. Note that the ionosphere is part of the atmosphere, but in this paper, for brevity, by the atmosphere is meant only the part lying below the ionosphere. The corresponding boundary conditions have the form

$$V\big|_{h=h_{\mathrm{I}}}=V_0\,,\quad V\big|_{h=h_{\mathrm{g}}(\lambda,\,\varphi)}=0, \tag{2}$$

where h is the height measured from sea level, the function $h_{\mathrm{g}}(\lambda,\,\varphi)$ sets the height of the Earth surface in geographical coordinates λ, φ; h_{I} is the height at which the ionospheric conductor originates. We also use Cartesian coordinates x, y, z for describing a local region when the curvature of the Earth surface can be neglected. We consider the ionospheric potential V_0 to be given.

Dirichlet boundary value problem (1, 2) has a unique solution. For the resulting field, we can calculate the total Joule dissipation, i.e. the value $\sigma\left(\mathrm{grad}\,V\right)^2$, integrated with respect to the atmosphere, it is finite. Mathematically, the atmosphere, similarly to a spherical layer, is a multiply connected domain. Generally speaking, this makes it difficult to formulate and examine the problems, but since we deal with Dirichlet boundary conditions (2), the proofs in the energy method are only slightly more complicated than those for a simply connected domain [Mikhlin, 1977].

The solution may have singularities, i.e. an infinite increase in the field strength if the given function $h_g(\lambda, \varphi)$ is not smooth. As an example, let us consider the electric field over a mountain ridge in an approximation that allows for an analytical solution. Let the axis of the cylindrical coordinate system be horizontal, the azimuthal angle α measured from the vertical, and ρ be the distance to the axis. Suppose the half-planes $\alpha=\pm\alpha_0$ are slopes of a mountain ridge. Since we are interested in the field only in a close vicinity of the edge $\rho=0$, we consider the air conductivity to be a constant. Then Equation (1) and second condition (2) take the form

$$\frac{1}{\rho}\frac{\partial}{\partial\rho}\left(\rho\frac{\partial V}{\partial\rho}\right)+\frac{1}{\rho^2}\frac{\partial^2 V}{\partial\alpha^2}=0,$$

$$V\big|_{\alpha=\pm\alpha_0}=0.$$

It is easy to find solutions for this problem, using the variable separation method.

$$V(\rho,\alpha)=v(\rho/\rho_0)^{\gamma_n}\cos(\gamma_n\alpha),$$

$$\gamma_n=(1+2n)\frac{\pi}{2\alpha_0},\ n=0,1,...$$

Drop solutions with negative n because they give an infinite potential at $\rho=0$. The constants v, ρ_0 provide normalization $V(\rho_0, 0)=v$, i.e. at an altitude ρ_0 vertically above the edge. The corresponding components and the squared electric field strength modulus have the form

$$E_\rho=-(\gamma_n v/\rho_0)(\rho/\rho_0)^{\gamma_n-1}\cos(\gamma_n\alpha),$$

$$E_\alpha=(\gamma_n v/\rho_0)(\rho/\rho_0)^{\gamma_n-1}\sin(\gamma_n\alpha),$$

$$E^2=(\gamma_n v/\rho_0)^2(\rho/\rho_0)^{2(\gamma_n-1)}.$$

For a mountain ridge $\pi/2<\alpha_0<\pi$, and for a valley between mountains $0<\alpha_0<\pi/2$. Accordingly, only γ_0 and only in the solution above the ridge can be less than 1, therefore only this solution has a singularity, i.e. infinite field strength at $\rho\to 0$. The Joule dissipation in the vicinity of $\rho<\rho 0$ is obtained by integrating σE^2. It turns out to be finite and independent of the inclination of the slopes $\sigma v^2\pi L/2$, where L is the length of the part of the ridge considered. Moving away from the edge, it is also finite since the conductivity and the electric field strength are finite there.

Unfortunately, we do not know a simple analytical solution of the problem near the peak of a conical mountain, where a singularity also appears. The singularities are smoothed out in the numerical solution of problems due to finite grid steps.

Our multigrid finite element method of solving this problem, which is based on minimizing the energy functional, is described in [Denisenko, Pomozov, 2010].

Test calculations including the ionosphere up to an altitude of 500 km suggest that it suffices to take $h_1=50$ km in order to almost not distort the field in the main part of the atmosphere. This allows us to restrict ourselves to the scalar air conductivity in this model. There is usually no data on the spatial distribution of air con-

ductivity. That is why we use the empirical model of the altitude distribution of conductivity regardless of horizontal coordinates, but with a land—sea difference. Figure 1 (left, bold curve) shows this distribution over land.

2. ONE-DIMENSIONAL MODEL

Ampferer et al. [2010] have shown that at horizontal scales $\gtrsim 100$ km we can use a one-dimensional model corresponding to verticality of atmospheric currents. Then the potential V in spherical coordinates r, $\pi/2-\lambda$, φ depends only on the radius r; therefore, boundary value problem (1), (2) reduces to solving a one-dimensional problem for r. It is easy to show that taking into account the sphericity of Earth in this equation makes a correction of less than 0.1 % to the current density and the resistance of the atmospheric column of interest. The sphericity can therefore be neglected, and the one-dimensional problem takes the form

$$\frac{d}{dh}\left(\sigma(h)\frac{dV(h)}{dh}\right)=0,\ V\big|_{h=h_I}=V_0,$$

$$V\big|_{h=h_0}=0,\tag{3}$$

where, strictly speaking, the function $V(h)$ must have indices λ, φ since it differs at each point with coordinates λ, φ (for brevity we do not write them); h_0 is the height $h_g(\lambda, \varphi)$ at the Earth surface point considered.

Solving this problem yields the vertical electric field strength $E(h)=-dV(h)/dh$ and the current density $j=-\sigma(h)dV(h)/dh$, which, in view of Equation (3), does not vary with height and hence is a function of only λ, φ. The latter circumstance makes it possible to reduce the solution of (3) to height integration

$$V_0=-j(\lambda,\varphi)\int_{h_0}^{h_1}dh/\sigma(h).$$

The integral of the given function is easy to calculate, this equality yields the value of $j(\lambda, \varphi)$ and the electric field strength, including the field near the Earth surface E_0. Also introduce a similar designation for conductivity σ_0. The relationship

$$R(\lambda,\varphi)=-V_0/j(\lambda,\varphi)=\int_{h_0}^{h_1}dh/\sigma(h)\tag{4}$$
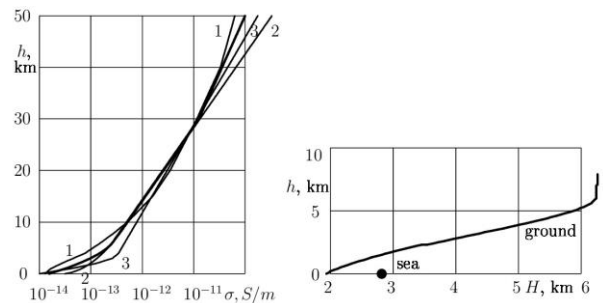

Figure 1. Vertical distribution of air conductivity (left). Thin lines: 1 — [Rycroft, Odzimek, 2010]; 2 — [Handbook of Geophys., 1960]; 3 — [Molchanov, Hayakawa, 2008]. The bold curve is [Denisenko et al., 2019]. On the right is the thickness of a homogeneous atmospheric conductor H (defined in Section 2) with the atmospheric conductivity model employed. The curve is over the land, the point is over the sea

has the meaning of the resistance of the atmospheric column with a cross-section of 1 m^2. In our model, it is determined only by h_0, but has a different uniform value for marine areas. Note that the atmosphere above 30 km adds ~0.3 % to $R(\lambda, \varphi)$.

The electric field strength near the Earth surface $E_0 = -V_0 / (R\sigma_0)$. Thus, in terms of the electric field strength and the current density near the Earth surface, the vertical air column is equivalent to a homogeneous column with constant conductivity σ_0 and thickness $H = R\sigma_0$. The parameter H can be called the thickness of a homogeneous atmospheric conductor above the surface point considered. With an exponential increase in conductivity with height $\sigma(h) = \sigma_0 \exp(h/H_0)$, the value of H is the same as in the exponent, $H=H_0$. In general, H is the characteristic altitude scale of an increase in conductivity.

Since the resistance of the atmospheric column R above plateaus and above the sea is less than above the low-lying land, the fair-weather current density is higher. According to Figure 1 (right), H increases with height of the surface, the electric field strength therefore decreases, i.e. the field strength and the current density change in antiphase.

The one-dimensional model was used in [Denisenko, Yakubailik, 2015] to find the total atmospheric conductivity; for doing this, $1/R(\lambda, \varphi)$ should be integrated throughout the planet. Nonetheless, when analyzing local phenomena, it gives a raw error, which is demonstrated below.

3. CONDUCTIVITY OVER LAND AND SEA

Figure 2 presents daily-seasonal diagrams of the fair-weather field constructed for the sea and land: the first is based on measurements made in [Harrison, 2013] during Carnegie Cruise VII [Denisenko et al., 2023], the second is based on field measurements at the Tomsk Observatory [Pustovalov et al., 2022].

Detailed similarity of the diagrams cannot be expected at least because the former is built using a smooth approximation of data, and the latter is more detailed and the month number on it refers to the middle of the month, whereas on the former m is the time from the beginning of the year in months. Nevertheless, comparing the dia-

grams shows that the ratio of field strengths over the low-lying land and the sea is ~2. According to the definition of the thickness of a homogeneous atmospheric conductor H given in the previous section, this can be interpreted as an approximate doubling of H during the transition from the low-lying land to the sea. The resulting ratio should be used to modify and update the air conductivity model. In our model, it is ~1.5. To increase it from 1.5 to 2, the conductivity near the ground should be increased more abruptly. This corresponds to the model developed in [Molchanov, Hayakawa, 2008]. At the same time, other profile parameters will have to be corrected in order to convey the characteristic relationships between the ground—ionosphere potential difference, surface conductivity, fair-weather field and current, which are embedded in the model [Denisenko et al., 2019]. Notice that there is a misprint in this article: in the formulas under Figure 4, which determine the altitude dependence of conductivity, the parameter s_0 must be positive.

4. RESULTS

As an example, the fair-weather field in the vicinity of Klyuchevskaya Sopka has been calculated. It is usually photographed in such a way that it seems to be a single volcano on the plain, but there are other volcanoes nearby that form a complex mountain system. A simplified model relief is depicted in Figure 3 (left). It is presented as five straight circular cones. Heights of peaks and inclination angles of slopes are approximately given although the craters of neighboring volcanoes are not taken into account. The cross-section of this mountain ridge along the parallel $y=-1.5$ km passing through the top of the volcano lies below the boundary of the region in Figure 4 and coincides with the hatched region in Figure 5.

The difference between the ground—ionosphere potentials $V_0=370$ kV is set so that the fair-weather field strength over the ocean is 120 V/m; over the low-lying land, ~180 V/m.

Boundary value problem (1, 2) was solved numerically. The method is described in [Denisenko, Pomozov, 2010]. The solution was actually in a horizontally limited region — large enough not to introduce errors in the atmospheric layer of interest.
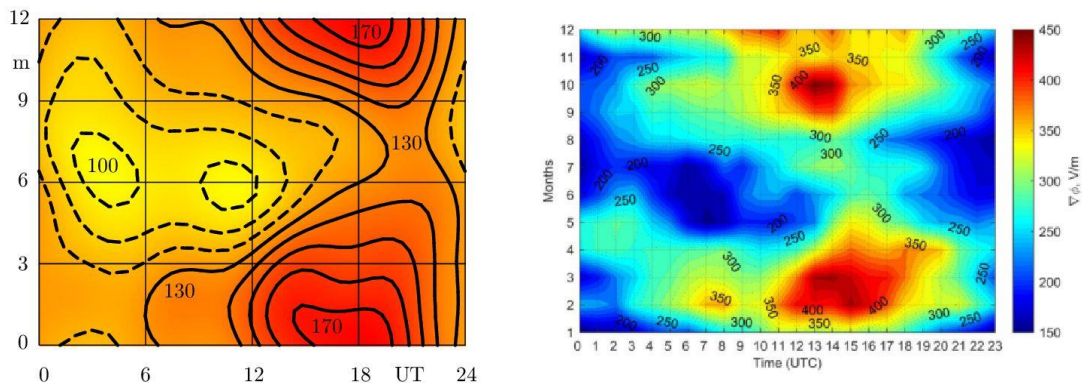

Figure 2. Daily-seasonal diagrams of the fair-weather electric field E_0 [V/m] over the sea (left) [Denisenko et al., 2023] (*m* — month) and over the land (right) [Pustovalov et al., 2022]
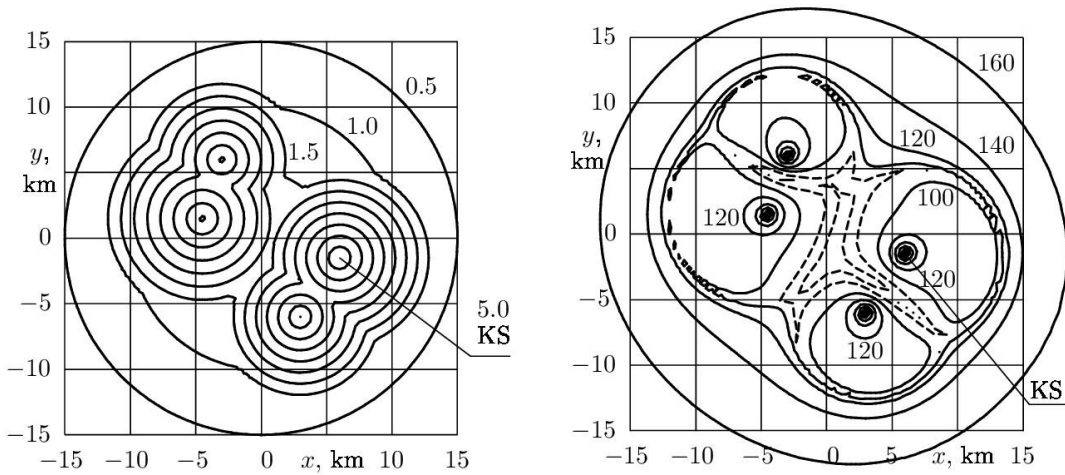
Figure 3. Model relief of the vicinity of Klyuchevskaya Sopka (left). Its peak is marked, the height is 5 km. The level lines are in increments of 0.5 km. On the right is the distribution of the vertical electric field strength component, —E_z, over the ground [V/m]; the level lines are in increments of 20 V/m
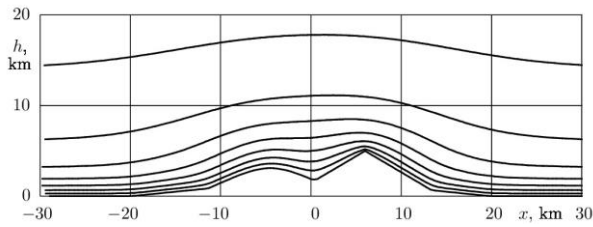

Figure 4. Equipotentials in the vertical cross-section above the parallel $y=-1.5$ km passing through the top of Klyuchevskaya Sopka; level lines are with increments of 50 kV
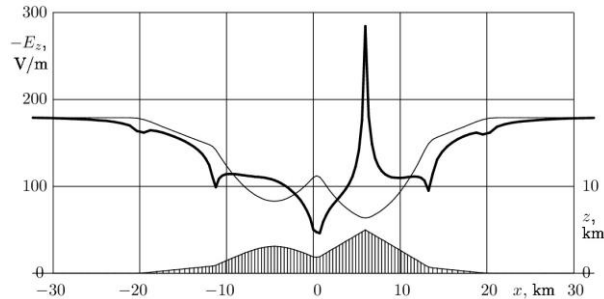

Figure 5. Distribution of the vertical electric field component over the ground along the parallel $y=-1.5$ km passing through the top of Klyuchevskaya Sopka. The bold curve is the result of a 3D calculation; the thin one is the 1D model. The hatched region with the height scale on the right is a cross-section of the model mountain range

Figure 3 (right) illustrates the distribution of the vertical electric field strength component $-E_z$ over the ground; level lines are drawn in increments of 20 V/m. To highlight the decrease in the field, dashed lines correspond to <100 V/m. As four peaks are approached, the field grows infinitely, but in calculations it is limited due to the finite grid step, as can be seen in Figure 5, which illustrates the distribution of the vertical electric field component over the ground along the parallel $y=-1.5$ km passing through the top of Klyuchevskaya Sopka. With distance from the mountains in the surrounding lowland plain, the field strength becomes as high as 179 V/m, which coincides with the field in the 1D model for the vertical air conductivity profile con-

sidered. Apparently, but for the close vicinities of the peaks, the field over the mountains decreases significantly compared to the field over the lowland.

Figure 4 shows the electric potential distribution in a vertical cross-section above the parallel $y=-1.5$ km passing through the top of Klyuchevskaya Sopka; level lines are with increments of 50 kV. The field decreases rapidly with altitude, from the difference between ground—ionosphere potentials $V_0=370$ kV, the first 350 kV are accumulated below 20 km. The field is seen to strengthen near the peak.

Figure 5 exhibits the resulting distribution of the electric field near the surface for the same cross-section. The natural properties of the electric field are visible: the field strength decreases in depressions and increases infinitely as it approaches the peak of the ideal cone. Due to the finiteness of the grid step, the field does not reach 300 V/m. In this calculation, the horizontal grid steps correspond to the hatching of the mountain cross-section, and the vertical steps in the main part of the domain are about three times smaller. The thin curve shows the result of the 1D model. In the 1D model, there are no depression—peak differences, there is only the height of the surface point above sea level considered. Note that the vertical field component is presented. Near the ground, it is smaller than the component normal to the surface since the surface is assumed to be equipotential (2). The difference is $\cos\alpha$ times, where α is the slope angle of the surface.

When the surface is flattened $\left(|x|>15\,\text{km}\right)$, the adequacy of the 1D model improves; and as horizontal surfaces far enough away from the mountains $\left(|x|>30\,\text{km}\right)$ are approached, the model becomes accurate. If measurements are made on the slope of the volcano at $x=10$ km, we obtain a fair-weather field strength of 109 V/m instead of 178 V/m on a plain at sea level with the same ionospheric potential and the same altitude curve of air conductivity. For such an observatory, calibration with the 1D model turns out to be quite accurate as opposed to measurements near depressions or peaks. At $x=11$ km,

even the coincidence of the results of the 3D and 1D models is accidentally obtained, and near $x=0$ they differ two-fold.

It is worthwhile taking into account this effect when analyzing measurements near Elbrus [Adzhiev et al., 2011], in Kamchatka [Akbashev et al., 2013], and in other mountainous areas.

Note that the fair-weather current density is less prone to fluctuations than the field strength since the field near the ground, even in the 1D model, is determined not only by the resistance of the atmospheric column as the current density is, but also by the conductivity in the surface layer. The latter changes significantly, for example, with dusting or radon emanation [Harrison et al., 2010]. Moreover, it is the current density that determines the effect of atmospheric electricity on the ionospheric electric field [Denisenko, et al., 2019]. It is therefore desirable to pay more attention to measuring the current density over the Earth surface. It is advisable to present the results of measurements of variations in current density and field strength in the form of daily-seasonal diagrams for each observatory. A comparison of such diagrams will clarify the generally accepted thesis about the planetary synchronicity of variations in the fair-weather field.

CONCLUSION

As the height of plateaus rises, the fair-weather current density increases, and the field strength decreases. This rule does not operate in the presence of steep mountain slopes. To include measurements of the fair-weather field in mountainous areas in the global field picture, it is useful to calibrate them, using the presented 3D model because the 1D model of atmospheric electric current continuity is not applicable for the relief with steep slopes. To clarify the calibration, it is desirable to know the specific features of the spatial distribution of air conductivity.

Comparing daily-seasonal diagrams of the fair-weather field shows that the field strength over the sea is about half as high as over low-lying land at the same time points.

REFERENCES

Adzhiev A.H., Boldyreff A.S., Dorina A.N., Kudrinskaya T.V., Kupovykh G.V., Novikova O.V., Panchishkina I.N., et al. Alpine atmospheric electricity monitoring and radon-222 measurement near Elbrus. *Proc. 14th Int. Conf. Atm. Electricity. Rio-de-Janeiro, Brazil,* 2011, pp. 112–115.

Akbashev R., Firstov P., Cherneva N. Recording of atmospheric electrical potential gradient in the central part of Kamchatka peninsula. *Solar-Terrestrial Relations and Physics of Earthquake Precursors 2013. E3S Web of Conferences,* 2013, vol. 62, 8620. DOI: 10.1051/e3sconf/20186202013.

Ampferer M., Denisenko V.V., Hausleitner W., Krauss S., Stangl G., Boudjada M.Y., Biernat H.K. Decrease of the electric field penetration into the ionosphere due to low conductivity at the near ground atmospheric layer. *Ann. Geophys.,* 2010, vol. 28, no. 3, pp. 779–787. DOI: 10.5194/angeo-28-779-2010.

Denisenko V.V., Pomozov E.V. Global electric fields in the Earth's atmosphere calculation. *J. Comp. Tech.* 2010, vol. 15, no. 5, pp. 34–50. (In Russian).

Denisenko V.V, Yakubailik O.E. The contribution of topography to the resistance of the global atmospheric conductor. *Solar-Terr. Phys.* 2015, vol. 1, no. 1, pp. 104–108. DOI: 10.12737/6044. (In Russian).

Denisenko V.V., Rycroft M.J., Harrison R.G. Mathematical simulation of the ionospheric electric field as a part of the Global Electric Circuit. *Surveys Geophys.* 2019, vol. 40, no. 1, pp. 1–35. DOI: 10.1007/s10712-018-9499-6.

Denisenko V.V., Rycroft M.J., Harrison R.G. Mathematical model of the global ionospheric electric field generated by thunderstorms. *Bulletin RAS: Phys.* 2023, vol. 87, no. 1, pp. 118–123. DOI: 10.3103/S1062873822700277.

Handbook of Geophysics. United States Air Force. NY: The Macmillan Company. 1960. 571 p.

Harrison R.G. The Carnegie Curve. *Surveys Geophys.* 2013, vol. 34, pp. 209–232. DOI: 10.1007/s10712-012-9210-2.

Harrison R.G., Aplin K.L., Rycroft M.J. Atmospheric electricity coupling between earthquake regions and the ionosphere. *J. Atmos. Solar-Terr. Phys.* 2010, vol. 72, pp. 376–381. DOI: 10.1016/j.jastp.2009.12.004.

Mareev E.A. Achievements and prospects of research of the global electric circuit. *Achiev. Phys. Sci.,* 2010, vol. 180, no. 5, pp. 527–534. DOI: 10.3367/UFNr.0180.201005h.0527.

Mikhlin S.G. Linear partial differential equations. M.: Higher School, 1977, 431 p.

Molchanov O., Hayakawa M. Seismo-electromagnetics and related phenomena: history and latest results. Tokyo: TERRAPUB. 2008, 189 p.

Pustovalov K., Nagorskiy P., Oglezneva M., Smirnov S. The electric field of the undisturbed atmosphere in the South of Western Siberia: a case study on Tomsk. *Atmosphere.* 2022, vol. 13, pp. 614–633. DOI: 10.3390/atmos13040614.

Rycroft M.J., Odzimek A. Effects of lightning and sprites on the ionospheric potential, and threshold effects on sprite initiation, obtained using an analog model of the global atmospheric electric circuit. *J. Geophys. Res.,* 2010, vol. 115, A00E37. DOI: 10.1029/2009JA014758.